Position and Speed Estimation for BLDC Motors Using Fourier-Series Regression

Ajit Basarur, **Jana Mayer**, **Antonio Zea**, and **Uwe D. Hanebeck**
Intelligent Sensor-Actuator-Systems Laboratory (ISAS)
Institute for Anthropomatics and Robotics
Karlsruhe Institute of Technology (KIT), Germany
jana.mayer@kit.edu, ajit.basarur@kit.edu, antonio.zea@kit.edu, uwe.hanebeck@kit.edu

***Abstract*—The control of brushless DC motors requires high-resolution angular position and accurate speed information. However, available sensor-based solutions only measure either the position or the speed directly, and then approximate the other numerically. In this work, a novel technique is presented to estimate both of these values simultaneously by sensing the stray magnetic field of the internal permanent magnets of the motor. However, achieving this requires the following two challenges to be addressed. First, the relationship between the magnetic field and the motor position is distorted by the rotational speed in a non-intuitive way, requiring careful modeling of these dependencies. Second, the derived model needs to consider that the angular position data is periodic by nature, but the magnetic field data and the angular speed data are linear (i.e., non-periodic). To achieve this, we introduce two different multidimensional regression models based on the Fourier series. Both models are first trained offline using reference data, and then used as a measurement function in a nonlinear estimator such as the EKF for online estimation. Evaluations show that both models outperform state-of-the-art techniques.**

I. Introduction

Brushless DC(BLDC) motors are a variant of Permanent Magnet Synchronous Motors (PMSM) that have found widespread applications because of their low maintenance, high efficiency, and lower susceptibility to mechanical wear. For efficient commutation under variable speed drive, this type of motors is operated using the Field-Oriented Control (FOC) algorithm [1], which requires both high-resolution angular position and accurate speed information for smooth operation [2]. However, available sensor-based solutions only provide either the position or the speed [3], [4] directly.

One of these sensor-based solutions consists of sensing the stray magnetic field of the BLDC motor [5] to obtain an estimate of the angular speed. This is achieved, for example, by counting the number of zero crossings [6], [7] of the signal. Although the speed information obtained from this method has some drawbacks [8], the underlying concept is still promising, especially because its only requirement is a low-cost magnetic sensor.

The stray magnetic field not only can be used for the speed estimation but also can be used for the position estimation of the BLDC motor. We propose to model the stray magnetic field measurement data obtained from a low-cost magnetic sensor and use it as a measurement function in a stochastic nonlinear filter to simultaneously estimate both the angular position and speed of the BLDC motor. However, this is not a straightforward task, in particular because we have to deal with three challenges. For illustration, we will use the example data taken from a real motor shown in Fig. 1. First, the observed shape of the magnetic field (Fig. 1a) cannot be described using a simple sinusoidal signal, as would be expected. These perturbations are caused by the winding coils and the motor housing (Fig. 1a, orange with coils, blue without). Second, the stray magnetic field is not only dependent on the angular position, but also on the operating speed of the motor. This is a sensor-related effect, and manifests both without coils (Fig. 1b) and with coils (Fig. 1c). Third, the mapping needs to consider that the angular position data is periodic by nature, whereas both the magnetic field data and the angular speed data are not.

A common approach for periodic signal regression is to use Fourier series [9], [10], which compactly express a given periodic signal with a set of harmonics in the frequency domain. The coefficients or the amplitudes of these harmonics can be stored in a vector of finite (and relatively small) size [11]. If the signal is non-periodic, then the Fourier transform can be applied instead of the Fourier series. However, the frequency domain representation of the non-periodic signal is continuous, and it cannot be expressed by a vector of finite size [11]. As we are dealing with a mapping that is periodic in one dimension and non-periodic in the other, regression approaches like multidimensional Fourier series [12], [13] cannot be used, because they require all the underlying data to be circular (i.e., periodic on a manifold). Furthermore, while there are several parametric multivariate linear-circular regression models in literature [14]–[18], these models make assumptions about the underlying distributions of the data, and furthermore, they are application-specific. Hence, they are not suitable for modeling the considered stray magnetic field.

To address these issues, we propose a hybrid model for the angular position (periodic) and speed (non-periodic) as follows. First, for a given set of support points in the speed domain, we model the relationship between the magnetic field signal and the positions with standard Fourier series. Then, for the speeds inbetween, we interpolate the values from nearby support points. This can be achieved using inverse distance weighting scheme [19], polynomial regression of the magnetic field values, or by interpolating the Fourier coefficients

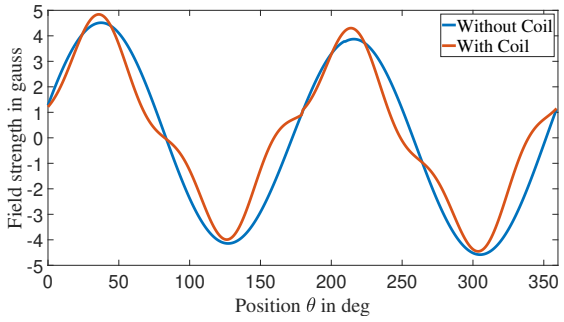

(a) Example of magnetic field strengths measured on a real motor, with and without coils at 500 RPM.

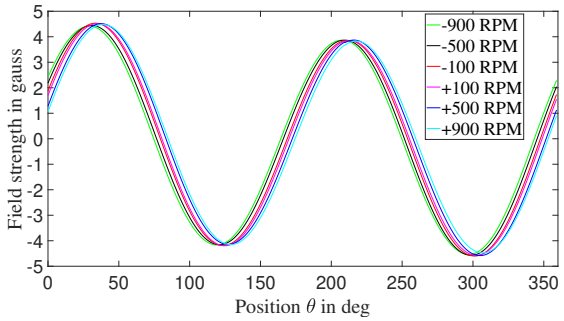

(b) Magnetic field dependency on different angular speeds of a BLDC motor without coils and housing.

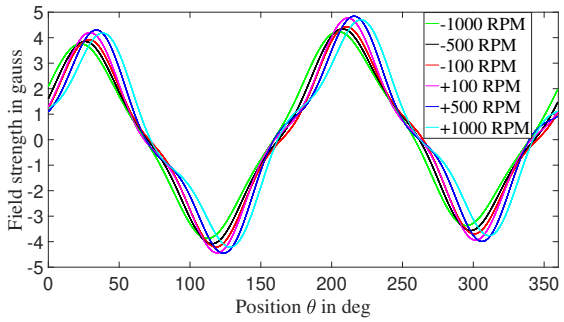

(c) Magnetic field dependency on different angular speeds of a BLDC motor with coils and housing.

Fig. 1: Stray magnetic field measurements of a real reference motor.

instead. The hybrid model is implemented in two steps. First, the Fourier coefficients and the interpolation parameters are trained offline, using experimental data consisting of known magnetic fields, positions, and speeds. Then, during online operation, the model parameters are assumed to be known, and the positions and speeds are estimated from the magnetic fields instead.

This paper is structured as follows. The next section formulates three important problems related to modeling and estimation. Sec. III proposes a two-stage approach for online estimation of the position and speed of BLDC motor. Sec. IV discusses the stray magnetic field modeling, which is the core part of this paper. The last two sections Sec. V and Sec. VI give an overview of the experiment setup and the evaluations.

II. Problem Formulation

In the following, we provide formulations for the three key problems we aim to solve. The first problem is to describe the physical issues responsible for the shapes in Fig. 1, to ensure that the results are reproducible. The second problem is to derive a parametric regression model that accurately describes the dependencies of the magnetic field. The third problem deals with the online estimation of the angular position and speed of the motor based on the derived model.

A. Shape and Dependencies of the Magnetic Field

As a motivating example, the stray magnetic field of a BLDC motor measured at $500\,\mathrm{RPM}$ is shown in Fig. 1a. The orange line is observed under normal operation of the motor. Then, we remove the coil and the housing of the motor, and drive it externally as shown in Fig. 6. The resulting magnetic field strength is drawn in blue. We observe that the shape of the magnetic field is sinusoidal if the coil and motor housing are absent. There are two similar cycles present in one complete mechanical rotation of the motor, indicating that the motor has four magnetic poles. Under normal operation of the motor, however, it can be easily seen that the magnetic field deviates from the sinusoidal shape with dips and surges at zero-crossings. This perturbation is attributed to the combined effect of the coil winding profile and the motor housing on the stray magnetic field of the rotor's permanent magnets.

Further experimental observations reveal the speed-dependent behavior of the magnetic field. In the absence of the motor housing and coils, only the speed-dependent phase shift occurs, as presented in Fig. 1b. Note that the shift is different for positive and negative speeds. This could be attributed to the combined frequency response of the magnetic sensor and the amplifier board. In the presence of housing and coils, a speed-dependent form change is observed in addition to the phase shift, shown in Fig. 1c. Overall, the magnetic field strength is not only dependent on the angular position but also on speed. Furthermore, the dependency is nonlinear.

B. Modeling the Dependencies

Based on the nonlinear dependencies of the magnetic field strength B on angular position θ and speed ω, the second problem that needs to be formulated is an adequate function that relates the three values. The first predictor variable θ is circular by nature and the second, ω, is linear. In the event of no speed-dependency, the Fourier series alone would be sufficient to model the magnetic field. However, in order to include the speed-dependent behavior, either an entirely different approach such as Gaussian Processes (GP) [20] or an extension to Fourier series is necessary. GPs are capable of modeling complex multivariate relationships but are computationally expensive, making approaches that extend Fourier series preferable due to their low computational cost. Therefore, we extend the series to accommodate ω, and provide a model function $B(\theta, \omega)$.

C. Online Estimation of Position and Speed

Using the modeled function $B(\theta, \omega)$, we will now describe the rotation system and measurement models. For the online estimation, we define the state of a running motor at the timestep k as $\underline{x}_k = [\theta_k, \omega_k]^T \in \mathbb{R}^2$, and assume that it evolves with each time-step following

$$\underline{x}_{k+1} = \boldsymbol{A}_k \cdot \underline{x}_k + \underline{w} \ , \tag{1}$$

where $\underline{w} \sim \mathcal{N}(\underline{0}, \boldsymbol{R})$ represents system noise. Assuming a constant velocity model, the system matrix $\boldsymbol{A}_k$ is given by

$$\boldsymbol{A}_k = \begin{pmatrix} 1 & \Delta T_k \\ 0 & 1 \end{pmatrix} \ , \tag{2}$$

where ΔT_k represents the timestep.

At a timestep k, the sensor placed near the motor measures the stray magnetic field b_k, which is mapped to the current state of the motor $\underline{x}_k$ using the measurement equation

$$b_k = h\left(\underline{x}_k\right) + v \ , \tag{3}$$

where $v \sim \mathcal{N}(0, \sigma_v^2)$ represents the measurement noise. The modeled function of the magnetic field defines the nonlinear function $h\left(\underline{x}_k\right) = B(\theta, \omega)$. If the sensor provides multiple measurements at one time step, e.g. different components of the magnetic field vector, they can be stacked into a vector.

III. Proposed Approach

We now describe our two-stage solution to estimate the angular position and speed of the electric motor in detail. This two-stage approach, combined with the experiment setup, is shown in Fig. 2. The experiment generates magnetic measurements B_x and B_y, but can also provide a reference angular position θ_r as a ground truth.

In the first stage, the relationship between $B_{x/y}$, θ_r, and ω is modeled offline by accumulating experimental data and training over them using regression techniques. For regression, two approaches are proposed. Both of the approaches are based on a Fourier series for the position variable and are extended for the speed variable. More details about modeling are provided in Sec. IV.

In the second stage, the learned model $B(\theta, \omega)$ is used as a nonlinear measurement function $h\left(\underline{x}_k\right)$ in (3) in order to estimate both the position and speed of the BLDC motor online. In this stage, the position and speed information are estimated every time step with the arrival of magnetic measurements. For online estimation, the Extended Kalman Filter (EKF) is used.

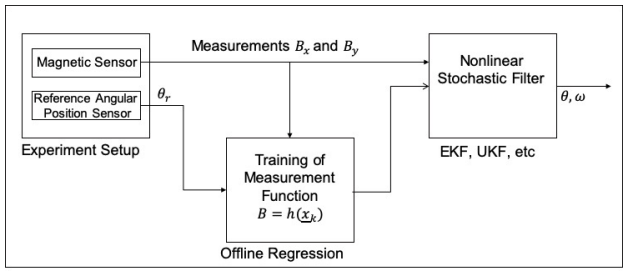

Fig. 2: Block diagram describing regression and filter.

IV. Modeling Approach

In general, a Fourier series is applied to one-dimensional periodic signals and spherical harmonics to multidimensional periodic signals. As described in Sec. II-B, the form of the magnetic field is not only dependent on θ but also on ω. The angular position is circular while the angular speed is linear. On that account, the application of a Fourier series is not straightforward. The modeling approach should consider this mixture of circular-linear data and should be computationally inexpensive. In addition, the experimental data is obtained only for a discrete set of speeds to reduce the size of the dataset. The proposed approach should be able to deal with such data sets.

To account for the experimental data, using a Fourier series for its simplicity, and modeling the magnetic field data such that computational cost is minimal, we propose two different approaches. The first approach couples Fourier series and the inverse distance weighting [19] interpolation technique. It is referred to as Fourier-Weighted Interpolation (FWI) in this paper. The second approach applies a Fourier series for θ and polynomial regression for ω on the experimental data. This approach is referred to as Fourier-Polynomial Regression (FPR) in this paper. In this section, we will first introduce the Fourier series, followed by FWI and FPR.

A. Fourier Series

Fourier analysis deals with the decomposition of a periodic signal into a weighted sum of sine and cosine functions, and their harmonics. Consider a periodic signal $B(\theta)$ of fundamental frequency λ

$$B(\theta) = a_0 + \sum_{n=1}^{N} \{a_n \cos(\lambda n \theta) + b_n \sin(\lambda n \theta)\} \ , \tag{4}$$

where a_0 is the mean of the signal and n is the harmonic number. For a given input-output datapair of size Q, $\{\theta_q, B_q\}$ where $q = 1, 2, \ldots, Q$, the estimation of Fourier coefficients is done using the linear least-squares technique provided that the parameter λ is pre-determined.

B. Fourier-Weighted Interpolation (FWI)

The dataset from the experiment setup is partitioned into multiple subsets with each of the subsets corresponding to a single speed. For each subset, then the magnetic field intensity for each of the subsets can be modeled using Fourier series as

$$\begin{aligned} B(\theta, \omega_1) &= f_1(\theta) \\ B(\theta, \omega_2) &= f_2(\theta) \\ &\vdots \\ B(\theta, \omega_M) &= f_M(\theta) \ . \end{aligned} \tag{5}$$

From the dataset, an $M-$tuple list is created $\big\{(\omega_1, f_1), (\omega_2, f_2), \cdots, (\omega_M, f_M))\big\}$. To find the interpolated

value at a given speed ω, the inverse distance weighting rule [19], suggests

$$B(\theta,\omega) = \frac{\sum_{i=1}^{M} g_i(\omega)\cdot f_i(\theta)}{\sum_{i=1}^{M} g_i(\omega)} \quad .$$

The weight g_i is an inverse of the absolute distance $|d|$ between ω and ω_i raised to power l

$$g_i(\omega) = \frac{1}{|d(\omega,\omega_i)|^l} \quad .$$

In this paper, we use the special case of inverse distance weighting with l equals one and two neighboring tuples such that $\omega_i < \omega < \omega_{i+1}$. This simplification leads to a standard weighted averaging technique. For a given speed ω that falls between the boundaries ω_i and ω_{i+1}, the magnetic field is a weighted sum of f_i and f_{i+1} given by

$$B(\theta,\omega) = g_i \cdot f_i + g_{i+1}\cdot f_{i+1} \quad . \tag{6}$$

And the weights are defined as

$$g_i = \frac{\omega_{i+1}-\omega}{\omega_{i+1}-\omega_i} \quad ,$$
$$g_{i+1} = \frac{\omega-\omega_i}{\omega_{i+1}-\omega_i} \quad .$$

It is possible to use more than two tuples for the interpolation. This has higher computational cost and the application of the derivative chain-rule to be used in the EKF setting.

C. Fourier-Polynomial Regression (FPR)

As the name suggests, this method interlinks the Fourier series and polynomial regression independently. The combination is done heuristically as a two-step approach at the beginning but leads to an analytic closed-form solution.

As the first step of the two-step approach, the Fourier series technique is applied to each subset and the coefficients are generated. The number of generated coefficients for each subset is equal as shown in Fig. 3. In the second step, polynomial regression of chosen degree p is applied to the Fourier coefficients. Denote a Fourier coefficient as $a_n^{\omega_m}$, where n corresponds to the harmonic number and ω_m to a particular speed.

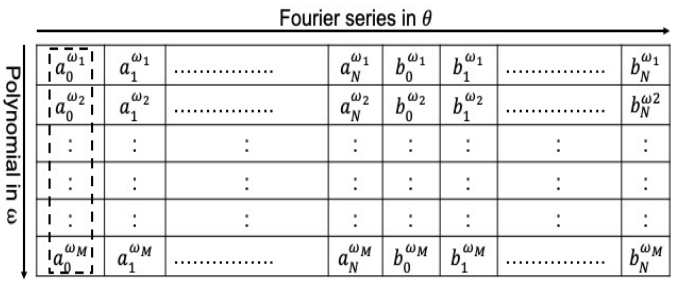

Fig. 3: Fourier-Polynomial fit illustration.

Applying Fourier series for the angular position θ and polynomial regression for the angular speed ω gives the Fourier-polynomial model in the following analytic form

$$B(\theta,\omega) = a_0(\omega) + \sum_{n=1}^{N}\{a_n(\omega)\cdot\cos(n\lambda\theta) + b_n(\omega)\cdot\sin(n\lambda\theta)\} \quad . \tag{7}$$

A set of Fourier coefficients representing the same harmonic number across different speeds is represented with pth degree polynomial in the following form

$$a_n(\omega) = c_n^0 + c_n^1\omega + c_n^2\omega^2 + \cdots + c_n^p\omega^p \quad ,$$
$$b_n(\omega) = d_n^0 + d_n^1\omega + d_n^2\omega^2 + \cdots + d_n^p\omega^p \quad ,$$

where c_n^j and d_n^j represent the jth polynomial coefficient of the nth Fourier harmonic for $a_n(\omega)$ and $b_n(\omega)$ respectively. Please note that for a given speed, i.e., if ω is constant, (7) is equivalent to (4).

c_n^j, d_n^j, and λ are the model parameters that need to be estimated. If the parameter λ is fixed, then the estimation reduces to a linear least-squares problem. The parameter λ corresponds to the fundamental frequency and it is fixed to $\frac{2\pi}{360}$ for our dataset.

In order to calculate the model parameters c_n^j and d_n^j, either a heuristic approach can be applied, or a Bayesian approach can be employed with the analytic form of (7).

V. Experiment Setup

For evaluating the proposed approach, we use the hardware setup schematically shown in Fig. 4. The main part of the setup is a 24 V BLDC motor [21] run with a corresponding controller board. The stray magnetic field of the motor is measured at the back of the motor with a two-axis Anisotropic MagnetoResistive (AMR) sensor HMC1052 [22]. The AMR sensor detects two orthogonal components of the magnetic field B_x und B_y. For a good Signal to Noise Ratio (SNR), the sensor was placed at an appropriate axial distance from the motor. Then, a suitable radial position was determined for the sensor where the field intensity produced from the internal permanent magnets is significant and measurable with the existing instrumentation amplifier. This corresponds to the

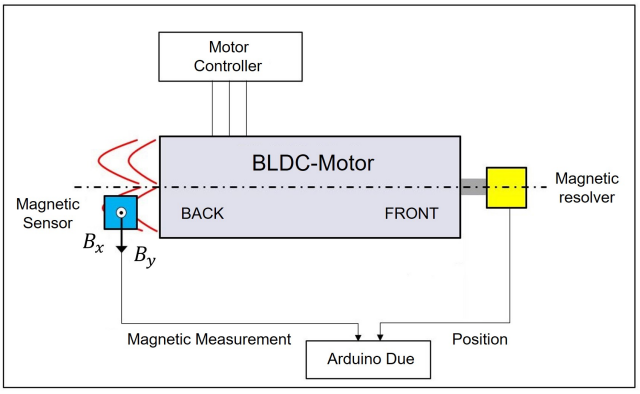

Fig. 4: Schematic illustration of hardware setup.

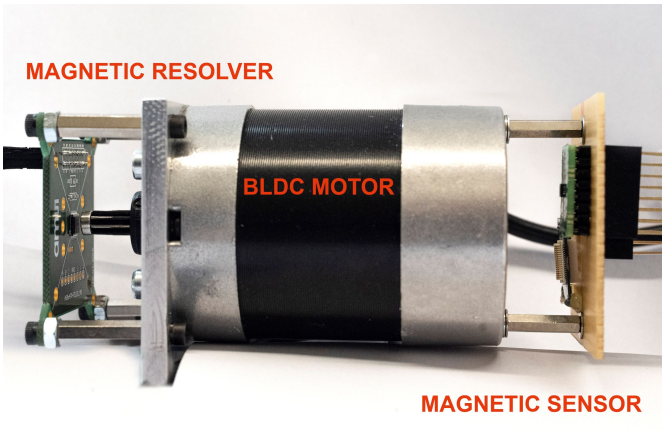

(a) BLDC motor with magnetic sensor and resolver.

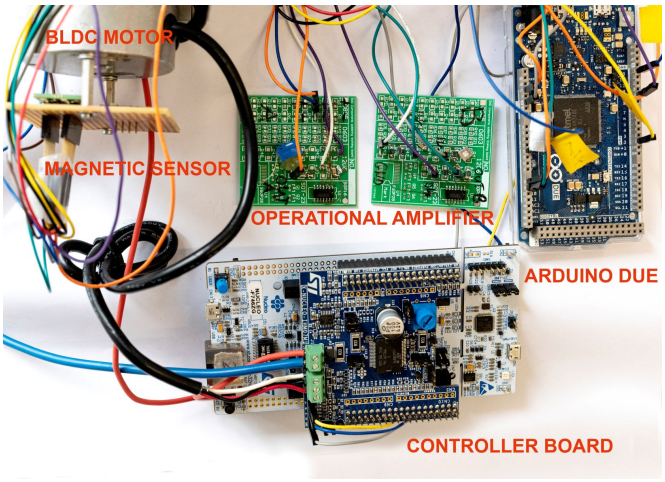

(b) Hardware components of the experiment setup.

Fig. 5: Hardware setup used for magnetic field measurements of a BLDC motor.

sensor being placed at a non-centered radial position between the axis of rotation and the circumference of the motor housing. For modeling, the ground truth angular position is obtained using a magnetic resolver [4]. Due to a lack of space, a speed sensor was not mounted, but instead, the angular speed was calculated on the basis of the measured angular position using a numerical differentiation [8]. The experiment setup is shown in Fig. 5 and all used hardware components are listed in table I. Using the experiment setup, magnetic field data were collected for different operating speeds of the motor. The measured field value in both directions is non-sinusoidal and dependent on the speed as well. The shape

TABLE I: Components of the experiment

Component	Hardware
Controller Board	Nucleo-F746ZG [23] and IHM07M1 [24]
Magnetic Sensor	HMC1052 Honeywell [22]
Magnetic Resolver	AS5047P [4]
Motor	24 V Brushless DC Motor [21]

deformation and phase lag changes due to speed have been already described in Sec. II. As the used BLDC motor has a four-pole rotor, the observed magnetic field has two sinusoidal-like cycles. Referring to Fig. 1 it can be clearly observed that the two cycles are not identical. This might be caused by either production inaccuracies of the rotor or the presence of non-identical magnets in the four-pole motor. These differences between the two cycles are even advantageous for the proposed approach as they lead to a reduction of ambiguity.

It is also important to consider the fact that by choosing a non-centered position of the sensor, the measured magnetic field components B_x and B_y are not $90°$ shifted versions of each other. In this manner, more information is available for estimating the angular position and speed.

Also, an additional experimental setup was created to observe the shape of the magnetic field without housing and coils as shown in Fig. 6. The motor housing and the coils were separated from the BLDC motor keeping the permanent magnets intact. This BLDC motor was driven externally at different speeds using another motor. The magnetic sensor was placed at the same location in order to compare the measurements from the other setup. The observed shape of the magnetic field for both experimental setups are shown in Fig. 1b.

In the next section, the data collected from the experiment is evaluated with our proposed approach.

VI. Evaluation

The proposed approach is evaluated using data generated with the hardware setup presented in Sec. V. As mentioned before, the angular position is measured with a magnetic resolver and the angular speed is calculated based on the position measurements. The corresponding magnetic field measurements consist of two orthogonal components B_x

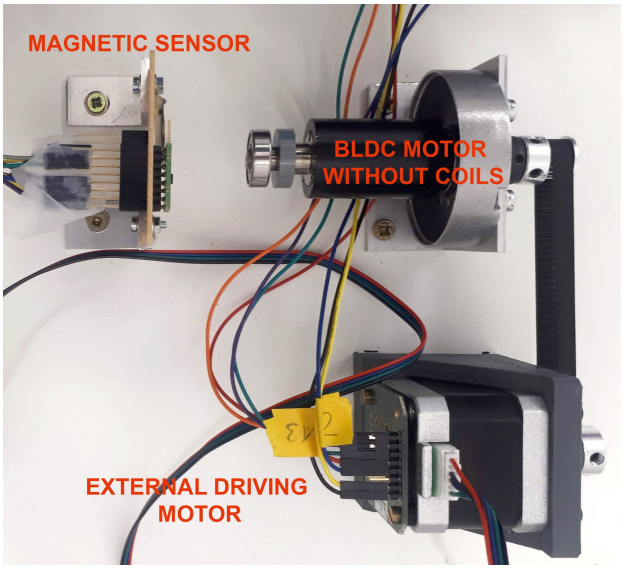

Fig. 6: Hardware setup used for magnetic field measurements of a BLDC without housing coils.

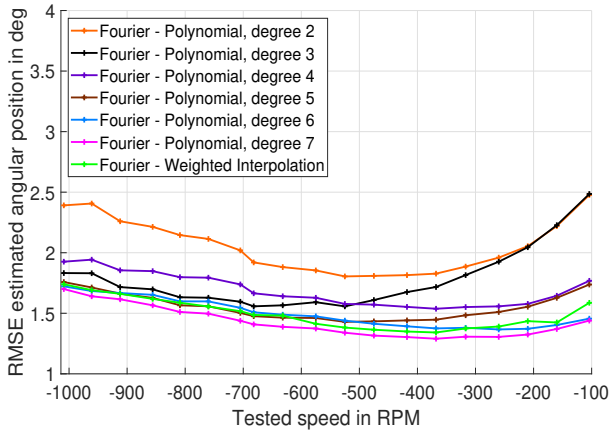

(a) Position estimation error for negative speeds.

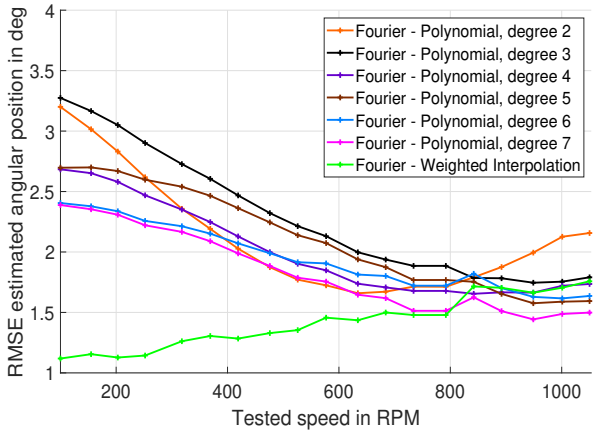

(b) Position estimation error for positive speeds.

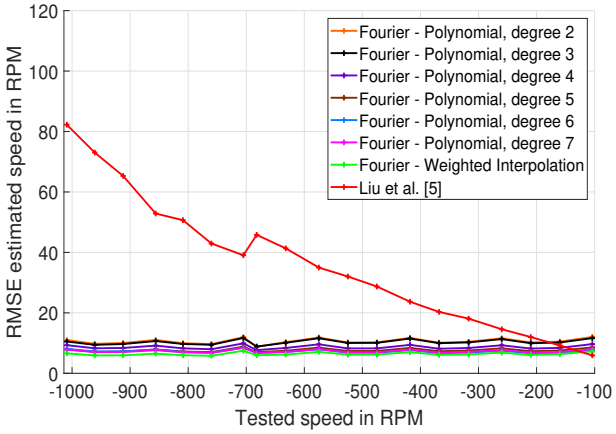

(c) Speed estimation error for negative speeds.

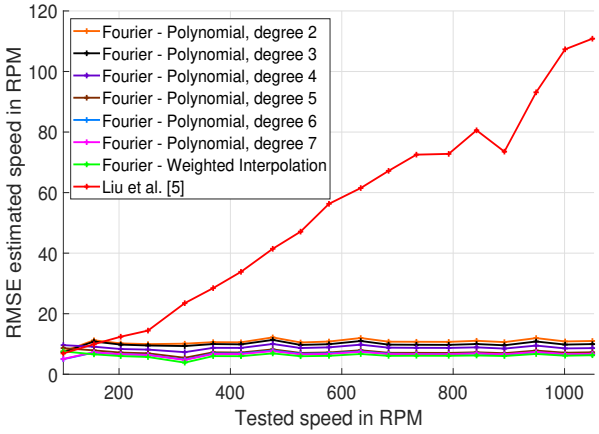

(d) Speed estimation error for positive speeds.

Fig. 7: Error of estimation for different operating motor speeds.

and B_y. For the evaluation, three separate individual data sets are recorded, one each for training, validation, and testing, respectively. In all sets, the magnetic field measurements are standardized by subtracting the mean and dividing by the standard deviation. The training set contains data for several constant speeds, more specifically for $[-4000, -3800, ..., -200, -50, 50, 200, ..., 3800, 4000]$ RPM.

Using the training set, the function $B(\theta, \omega)$ is modeled. As the first step, for each speed, the magnetic field is modeled by applying the Fourier series with seven harmonics taken into account. In the second step, the two methods proposed in Sec. IV-B and Sec. IV-C are applied. The FWI method was implemented with two neighboring speed data sets. FPR was applied with a heuristic approach as it is straight-forward and simple to calculate. The modeled function served as a measurement function in the EKF for online estimation. For the EKF, we used the framework provided in the Nonlinear Estimation Toolbox [25]. The measurement function $h(\underline{x}_k)$ and the corresponding Jacobian matrix calculation are custom implementations that are plugged into the EKF framework.

The measurement noise is determined experimentally. For a given speed, the data is segmented into multiple bins with $0.5°$ width. The width is chosen small as the sinusoidal signal has high gradients at zero crossings. The calculation of the mean and standard deviation for each bin show a dependence of the measurement noise on both the angular position and speed. Nevertheless, to avoid further calculation expenses, the measurement noise is approximated by its mean over all angular positions and speeds. The determined measurement noises for the two magnetic field components are $\sigma^2_{v,B_x} = 0.0073\,\mathrm{Gs}^2$ and $\sigma^2_{v,B_y} = 0.0060\,\mathrm{Gs}^2$ respectively. The system noise matrix $\boldsymbol{R}$ was adjusted manually for every model employing the validation data set. The obtained values are given in table II.

For testing, we used two data sets with stepwise changing speeds, one from -1000 to -100 RPM and the other from 100 to 1000 RPM. The estimation quality was evaluated separately for each speed. The results are presented in Fig. 7. For both the angular position and speed, the Root Mean Square Error (RMSE) between the estimated values and the ground truth is given in the graphs.

TABLE II: System noise used in evaluation.

Model	$\boldsymbol{R}$ in $\left[\mathrm{rad}^2\ {}^{\mathrm{rad}^2}/_{\mathrm{s}};\ {}^{\mathrm{rad}^2}/_{\mathrm{s}}\ {}^{\mathrm{rad}^2}/_{\mathrm{s}^2}\right]$
Fourier - Polynomial Regression (FPR), degree 2	$\mathrm{diag}(0.016^2, 0.19^2)$
Fourier - Polynomial Regression (FPR), degree 3	$\mathrm{diag}(0.021^2, 0.23^2)$
Fourier - Polynomial Regression (FPR), degree 4	$\mathrm{diag}(0.003^2, 0.38^2)$
Fourier - Polynomial Regression (FPR), degree 5	$\mathrm{diag}(0.030^2, 0.63^2)$
Fourier - Polynomial Regression (FPR), degree 6	$\mathrm{diag}(0.011^2, 0.80^2)$
Fourier - Polynomial Regression (FPR), degree 7	$\mathrm{diag}(0.004^2, 0.78^2)$
Fourier - Weighted Interpolation (FWI)	$\mathrm{diag}(0.290^2, 0.76^2)$

The results of the position estimation are shown in Fig. 7a for the negative speed range and in Fig. 7b for the positive speed range. For negative speeds FPR tends to perform better using higher polynomial degrees. FWI shows similar results to FPR with degree five and six. Only FPR with degree seven outperforms FWI over the whole negative speed range. Positive speeds using FPR with higher polynomial degrees also show mostly better performance. FWI performs significantly better than all FPR models for positive speeds up to $750\,\mathrm{RPM}$. Evaluating the regression quality we see that FWI models the magnetic field better than FPR for lower positive speeds. The reason is a faster magnetic field change in those speed ranges, as do some of the Fourier coefficients. These fast changes are modeled better with FWI as it takes only the neighboring speed data sets into account. FPR is not able to follow those local changes due to its smoothing property.

For speed estimation, Fig. 7c and Fig. 7d, FWI performs best. The estimation using FPR gets more accurate with increasing polynomial degree. All models show a nearly constant quality over the complete speed range. In addition, we compare our results with the zero-crossings method presented by Liu et al. [5]. The error of the estimation using the zero-crossings method increases with speed. The reason might be a lower resolution in detecting the zero-crossings at higher speed. Beyond $200\,\mathrm{RPM}$ all of our models and above $150\,\mathrm{RPM}$ some of our models show better performance than the zero-crossings method. Especially for higher speeds, our approaches are much more accurate.

Overall, Fourier-Weighted Interpolation (FWI) produced the best results for both position and speed estimation over the range of operating speeds. In Fourier-Polynomial Regression (FPR) higher polynomial degrees resulted in better performance.

VII. Summary, Conclusion and Future Work

In this paper, position and speed of a BLDC motor were estimated by harvesting the stray magnetic field produced from the permanent magnets of the BLDC motor. This was achieved via a two-stage approach, namely offline stage and online stage. The offline stage dealt mainly with the modeling problem that established mapping between the magnetic field, the angular position, and the angular speed of the BLDC using Fourier-Weighted Interpolation (FWI) and Fourier-Polynomial Regression (FPR). The online stage uses the model developed in the offline stage as a measurement function in a nonlinear stochastic filter setting such as the EKF to simultaneously estimate both the position and speed of the BLDC for every magnetic sensor measurement.

Both approaches, FWI and FPR, are based on Fourier series due to the periodic nature of angular position but require extensions due to the non-periodic nature of speed. FWI consumes more memory space compared to FPR that compresses Fourier coefficients through polynomial regression. The evaluation of experimental data showed that FWI is in general better than FPR, unless a higher-degree polynomial is used for regression. Higher-degree polynomials are not recommended due to overfitting problems. In general, both approaches estimate high-resolution position information and accurate speed information. The speed estimation is much more accurate than the current state-of-the-art approach [5].

In the future, we would like to test FWI for multiple tuples to evaluate its performance against the existing two-tuple local approach. Furthermore, we plan to expand the existing data set to increase speed granularity and check the performance of FPR against FWI. For dense speed data sets, the number of coefficients to be stored is higher, and therefore FPR plays a key role in the reduction of the total number of coefficients and memory space.

Acknowledgment

This work was partially supported by the German Research Foundation (DFG) under grant HA 3789/17-1 and by the Ministry of Economic Affairs, Labour, and Housing of the state Baden-Wuerttemberg, Germany.

References

[1] S. Lee, T. Lemley, and G. Keohane, "A Comparison Study of the Commutation Methods for the Three-phase Permanent Magnet Brushless DC Motor," in *Proceedings of the Electrical Manufacturing Technical Conference 2009: Electrical Manufacturing and Coil Winding Expo, EMCWA*, Nashville, TN, United States, Sep. 2009.

[2] F. B. Cakar, "Optimal BLDC Motor Control for Autonomous Driving of RC Cars," Ph.D. dissertation, TU Wien, Wien, Nov. 2017.

[3] Trinamic, "Trinamic Optical Encoder TMCS-28," 2019. [Online]. Available: https://www.trinamic.com

[4] Ams AG, "Ams as5047u - High Resolution Rotary Position Sensor," 2019. [Online]. Available: https://ams.com/as5047u

[5] L. C. Liu, X. and P. Pong, "Velocity Measurement Technique for Permanent Magnet Synchronous Motors Through External Stray Magnetic Field Sensing," *IEEE Sensors Journal*, vol. 18, no. 10, pp. 4013–4021, 2018.

[6] L. Mažeika and L. Draudviliene, "Analysis of the Zero-Crossing Technique in Relation to Measurements of Phase Velocities of the Lamb Waves," *Ultragarsas (Ultrasound)*, vol. 65, no. 2, p. 7–12, 2010.

[7] D. Grillo, N. Pasquino, L. Angrisani, and R. Schiano Lo Moriello, "An Efficient Extension of the Zero-Crossing Technique to Measure Frequency of Noisy Signals," in *Proceedings of the 2012 IEEE International Instrumentation and Measurement Technology Conference*, Graz, Austria, May 2012.

[8] R. Merry, M. van de Molengraft, and M. Steinbuch, "Velocity and Acceleration Estimation for Optical Incremental Encoders," *Mechatronics*, vol. 20, no. 1, pp. 20–26, Feb. 2010.

[9] E. W. Weisstein, "Fourier Series." [Online]. Available: https://mathworld.wolfram.com/FourierSeries.html

[10] V. B. Haykin, S.S., *Signals and Systems*. Wiley, 1999.
[11] L. Chaparro, *Signals and Systems Using MATLAB*, 2nd ed. Academic Press, 2015.
[12] F. Pfaff, G. Kurz, and U. D. Hanebeck, "Multivariate angular filtering using fourier series," *Journal of Advances in Information Fusion*, vol. 11, no. 2, pp. 206–226, December 2016.
[13] A. Zygmund, *Trigonometric Series*, 3rd ed. Cambridge University Press, 2003, vol. 1 and 2.
[14] W. T. Johnson, R.A., "Some Angular–linear Distributions and Related Regression Models," *Journal of the American Statistical Association*, vol. 73, no. 363, pp. 602–606, 1978.
[15] A. SenGupta and F. I. Ugwuowo, "Asymmetric Circular-Linear Multivariate Regression Models With Applications to Environmental Data," *Environmental and Ecological Statistics*, vol. 13, no. 3, pp. 299–309, Sep. 2006.
[16] A. S. Sungsu Kim, "Regressions Involving Circular Variables: An Overview," in *Proceedings of Platinum Jubilee International Conference on Applications of Statistics (PJICAS)*, Kolkata, India, Dec. 2016.
[17] N. I. Fisher and A. J. Lee, "Regression Models for an Angular Response," *Biometrics*, vol. 48, no. 3, pp. 665–677, 1992.
[18] Z. J.-S. Qin, X. and X.-D. Yan, "A Nonparametric Circular–linear Multivariate Regression Model with a Rule-of-thumb Bandwidth Selector," *Computers & Mathematics with Applications*, vol. 62, no. 8, pp. 3048–3055, 2011.
[19] D. Shepard, "A Two-Dimensional Interpolation For Irregularly-Spaced Data," in *Proceedings of the 1968 ACM National Conference*, New York, NY, USA, Aug. 1968.
[20] A. Basarur, J. Mayer, M. Petrova, F. Sordon, A. Zea, and U. D. Hanebeck, "Position and Speed Estimation of PMSMs Using Gaussian Processes (to appear)," in *Proceedings of the 21st IFAC World Congress (IFAC 2020)*, Berlin, Germany, July 2020.
[21] "BLDC Motors with Planetory Gearbox." [Online]. Available: de.aliexpress.com/item/32796902315.html
[22] Honeywell, "1, 2 and 3 Axis Magnetic Sensors HMC1051/HMC1052/HMC1053," 2019. [Online]. Available: https://www.sparkfun.com/datasheets/IC/HMC105X.pdf
[23] "NUCLEO-F746ZG," library Catalog: www.st.com. [Online]. Available: https://www.st.com/en/evaluation-tools/nucleo-f746zg.html
[24] "X-NUCLEO-IHM07M1," library Catalog: www.st.com. [Online]. Available: https://www.st.com/en/ecosystems/x-nucleo-ihm07m1.html
[25] J. Steinbring, "The Nonlinear Estimation Toolbox," 2017. [Online]. Available: bitbucket.org/nonlinearestimation/toolbox